Science and Technology Indonesia
e-ISSN:2580-4391 *p*-ISSN:2580-4405
Vol. 11, No. 2, April 2026

Research Paper

Valorization of Palm Empty Fruit Bunch-Derived K_2CO_3 Catalyst: Structural Analysis and Application in Biodiesel Production

Susila Arita[1], Reno Fitriyanti[2,3*], Leily Nurul Komariah[1], Fitri Hadiah[1]

[1]*Department of Chemical Engineering, Sriwijaya University, Palembang, South Sumatera, 30139, Indonesia*
[2]*Doctoral Program in Engineering Science, Sriwijaya University, Palembang, South Sumatera, 30139, Indonesia*
[3]*Department of Chemical Engineering, PGRI Palembang University, Palembang, South Sumatera, 30116, Indonesia*
***Corresponding author**: renofitriyanti@ymail.com

Abstract
This study investigates the synthesis and performance of a K_2CO_3 catalyst derived from oil palm empty fruit bunch (EFB) ash for sustainable biodiesel production. X-ray Diffraction (XRD) revealed a dominant K_2CO_3 crystalline phase, while X-ray Fluorescence (XRF) confirmed a high potassium content (>40%). Despite its low surface area (0.11 m^2/g), the catalyst demonstrated high transesterification activity, achieving an optimal biodiesel yield of 85.89% with 3 grams of catalyst. Its high thermal stability, strong base sites, and macroporous structure all contributed to enhanced catalytic efficiency. Sustainability and techno-economic assessments indicate the catalyst's potential to reduce production costs, utilize biomass waste, and lower greenhouse gas emissions. Thus, the EFB ash-based K_2CO_3 catalyst shows significant promise for supporting environmentally friendly biodiesel production and contributing to the transition to a green economy and renewable energy.

Keywords
Valorization, Palm Empty Fruit Bunch (PEFB), K_2CO_3 Catalyst, Catalyst Characterization, Biodiesel Production, Transesterification

Received: 22 September 2025, Accepted: 16 January 2026
https://doi.org/10.26554/sti.2026.11.2.420-435

1. INTRODUCTION

Energy is a key driver of economic growth and production activities worldwide, making the sustainability of the global economy highly dependent on the stability of the energy supply (Wang et al., 2024). However, the use of fossil fuels leads to the emission of harmful pollutants that contribute to environmental degradation (Khan et al., 2023) and global warming (Rahman et al., 2024). Given the impacts of fossil fuel use, the use of new renewable energy and the development of sustainable energy resources are a necessity.

In recent years, global attention to climate change issues and the dependence on fossil fuels have encouraged researchers and industry to explore alternative, sustainable energy sources. Dependence on fossil fuels has led to the depletion of petroleum reserves from fossil sources; therefore, the facts indicate that research on renewable fuels or biofuels needs to be developed (Buchori et al., 2024). One alternative energy source that is environmentally friendly, renewable, and has excellent potential for development is biomass (Ahmad et al., 2023; Reddy, 2023). This source can be processed into various types of fuels, such as biodiesel (Garg et al., 2023). The use of biodiesel has several advantages over fossil fuels, including its biodegradability, non-toxicity, and low emissions (Awosusi et al., 2022; Mohammed, 2023; Moreira, 2023). The abundant availability of raw materials makes biodiesel a promising alternative to petroleum fuel.

Biodiesel, also known as fatty acid methyl ester (FAME), can be obtained through the chemical reaction of feedstocks derived from both vegetable oils and animal fats, as well as alcohols, using various methods, including transesterification, direct use, blending, microemulsion, and pyrolysis (Bhatia et al., 2020; Ismaeel et al., 2024). In general, the biodiesel production process can be carried out through the transesterification stage. Among the various methods, transesterification is the most common and extensively investigated reaction in biodiesel synthesis, employing alkaline earth metal oxides as solid base catalysts (Sulaiman et al., 2020). Compared to other biodiesel production methods, transesterification is the most commonly used method because it offers high productivity and efficient production costs (Athar and Zaidi, 2020), and produces biodiesel that exhibits properties similar to those of conventional diesel fuel (Karmakar et al., 2022). Traditionally, biodiesel is produced through the transesterification of vegetable oils or animal fats using homogeneous acid or base catalysts, such as NaOH, KOH, or H_2SO_4, dissolved in

methanol. However, homogeneous catalysts present several drawbacks, including difficulty in separating them from the reaction mixture, their single-use nature, and the generation of liquid waste that poses environmental concerns (Widianingsih et al., 2024). The transesterification method is considered the most technically efficient; however, the production process is strongly influenced by the type and quality of the catalyst used (Zahan and Kano, 2019; Hazrat et al., 2024).

Potassium carbonate (K_2CO_3), a strong base, has shown effective catalytic performance in biodiesel production. However, the high cost of pure chemical-grade K_2CO_3 limits its widespread use, especially in biodiesel production. Empty Palm Oil Bunches (EFB), which is the most significant amount of solid waste in the palm oil industry, where one ton of Fresh Fruit Bunches (FFB) processed can produce 23-30% of EFB waste. Data on the estimated utilization of EFB waste show that 73.4% remains waste and has not been utilized. EFB contains many potassium and carbon-based compounds, making it a potential raw material for the synthesis of K_2CO_3-based catalysts. The utilization of EFB as a catalyst not only offers a solution for waste management but also supports efforts to substitute expensive commercial catalysts with more economical and environmentally friendly alternatives (Laskar et al., 2018; Ibrahim et al., 2019). Not only does it reduce the environmental burden, but it also adds economic value to palm oil by-products and offers a greener approach to biodiesel synthesis (Atadashi et al., 2011; Ao et al., 2023).

Several studies have demonstrated that EFB ash contains alkaline compounds, such as K_2O, which can serve as a potassium source in heterogeneous catalysts (Balajii et al., 2019). Heterogeneous catalyst modification techniques, such as the impregnation of active substances like KOH or H_3PO_4, have been demonstrated to increase biodiesel conversion significantly (Basumatary et al., 2023). Even the use of KOH-impregnated EFB ash catalyst has achieved a conversion efficiency of up to 99.45% and meets European biodiesel standards (Yaakob et al., 2012).

Although previous studies have explored the use of EFB as a source of alkali compounds for the synthesis of potassium-based heterogeneous catalysts, most of these studies are still limited to the direct utilization of ash without extracting or identifying the active compounds contained therein in detail. In addition, previous studies using K_2CO_3 as a biodiesel catalyst generally relied on pure or analytical-grade K_2CO_3 (≥99%, Merck) as raw material, rather than K_2CO_3 sourced from EFB biomass waste. These studies generally focused on evaluating catalytic performance in transesterification reactions. However, they did not provide an in-depth understanding of the crystal structure, surface morphology, elemental composition, and specific surface area of K_2CO_3 compounds derived from natural sources of EFB ash.

Building on previous studies, this study focused on extracting K_2CO_3 compounds from EFB ash and conducted a comprehensive analysis of its structural characteristics using XRD, SEM, XRF, and SAA/BET tests. This approach provides a new perspective in linking the microscopic structure, elemental composition, and potential catalytic activity of EFB-extracted K_2CO_3, which has not been widely reported in the literature. Thus, this study confirms the potential of EFB waste as a high-value-added natural source of K_2CO_3 and provides fundamental characterization data for the development of biomass-based heterogeneous catalysts. The novelty of this research lies in its in-depth analytical approach to the structure and composition of K_2CO_3 extracted from EFB waste, not merely its use as a catalyst, thereby contributing to the development of more economical, environmentally friendly, and sustainable catalyst materials.

2. EXPERIMENTAL SECTION

2.1 Materials

The materials used in this study included Refined Bleached Deodorized Palm Oil (RBDPO; PT Sumi Asih, Bandung Regency, West Java, Indonesia), which was used as received as the biodiesel feedstock (100 g per batch). Technical methanol (70% v/v; Smart Lab, Indonesia) was used as the alcohol reagent at a mass ratio of 100 g oil to 30 g methanol. Empty fruit bunch (EFB) biomass was obtained from PT Perkebunan Nusantara VII (South Sumatra, Indonesia) and used as the raw material for catalyst preparation. Pure potassium carbonate K_2CO_3; Merck, Germany, ≥99%, pro analysis grade) was used for comparison. All other reagents and solvents used for analysis were of pro-analytical grade (Merck, Germany) and were obtained from a chemical distributor.

2.2 Methods

2.2.1 Preparation of EFB-Derived K_2CO_3 Catalyst

The catalyst was prepared from EFB using the following steps. First, the EFB was chopped and dried in the sun for one week. After drying, the EFB was burned in a furnace at 500-600°C for one hour (Komariah et al., 2024). The air flow entering the furnace was controlled to ensure the desired temperature could be maintained. The ash from combustion is then sieved and filtered using a 100-mesh sieve.

The extraction process of K_2CO_3 from EFB ash was carried out using the water dissolution method to obtain a solution rich in Potassium. A total of 100 grams of EFB ash was mixed with 700 mL of distilled water (solid to solvent ratio 1:7 (w/v)) and then stirred constantly at 60°C for 90 minutes to dissolve potassium-containing compounds. The mixture was then filtered using Whatman No. 42 filter paper to separate the insoluble solid residue. The filtrate obtained was evaporated on a hot plate until almost dry, then dried in an oven at 200°C for 18 hours to obtain the extraction solid. The dry solid was then finely ground and stored in a desiccator as the K_2CO_3 catalyst extracted from EFB ash. The extraction procedure employed in this study was adapted from the research group of the corresponding author, utilizing the optimum conditions previously determined in their study: a solid-to-solvent ratio of 1:7 (v/v), an extraction temperature of 60°C, and a stirring time of 90 minutes.

2.2.2 Catalyst Characterization Techniques

Properties of the prepared catalyst were investigated using standard methods, as previously applied in identifying EFB ash as a catalyst (Ibrahim et al., 2019; Komariah et al., 2024), and commonly employed in studies on biomass-derived catalysts (Arumugam and Sankaranarayanan, 2020; Aleman-Ramirez et al., 2021; Kanwal et al., 2025). Catalyst characterization was conducted to determine the catalytic properties of K_2CO_3 produced from EFB ash extract, utilizing XRD, SEM, and XRF techniques. An X-ray Diffraction analyzer was used to identify the crystalline phase formed and the crystal structure of the catalyst. The x-ray diffraction patterns were obtained using a Bruker AXS D8 Advanced diffractometer, equipped with nickel filtration and Cu Kα radiation (λ = 1.5406 Å). Surface morphology and elemental composition were examined by using a Scanning Electron Microscope SEM-EDX instrument (COXEM, Korea/(NeoScope^{TM} JCM-7000) and EDX detector (JEOL JED-2300). Elemental composition analysis and constituent compounds were determined by using an X-MET handheld X-Ray Fluorescence (XRF) analyzer.

2.2.3 Evaluation of Catalytic Activity

The activity of K_2CO_3 was investigated for the transesterification of RBDPO with methanol in a 250 mL round-bottom flask equipped with a reflux condenser and thermometer, placed on a hot plate with a magnetic stirrer. RBDPO (100 g), K_2CO_3, and methanol (30 g) were introduced into the reactor. The esterification efficiency was investigated at different catalyst levels (3, 6, 9, and 12 g). The reaction was carried out at 65°C for 4 hours with constant stirring of 450 rpm (Komariah et al., 2024; Salam et al., 2024). After the reaction was completed, the mixture was allowed to stand to separate biodiesel and glycerol. The biodiesel obtained was washed with warm water to remove the remaining catalyst and glycerol in the methyl ester. Washing is done using distilled water repeatedly until a transparent layer of water is obtained. The biodiesel was then dried for 1 hour at 100°C and analyzed. Each transesterification experiment was conducted three times under the same operating conditions to ensure reproducibility of results. The reported biodiesel yield values represent the average of three repetitions.

2.2.4 Biodiesel Product Analysis

Biodiesel produced from the transesterification process with K_2CO_3 catalyst from EFB ash was analyzed using Gas Chromatography -Mass Spectrometry (GC-MS) type Shimadzu QP 2010 SE with FID and MS detector with test environment conditions at 25°C, 68% humidity to determine the methyl ester composition. The physical properties of the biodiesel produced were also tested, including viscosity, density, acid number, total glycerol content, and biodiesel yield, to be compared with the ASTM standards.

3. RESULTS AND DISCUSSION

3.1 Characterization of Catalysts K_2CO_3 From EFB Ash

3.1.1 XRD Analysis

The crystal structure and phase composition of the K_2CO_3 catalyst were analyzed using the X-ray diffraction (XRD) technique to identify the crystalline compounds contained in the material. XRD is one of the most effective characterization techniques for identifying and analyzing the composition of substances and their crystal structure (Bo et al., 2025). The XRD technique is used to analyze the X-ray diffraction pattern produced when X-rays interact with a sample. X-ray diffraction patterns were obtained using a Rigaku MiniFlex 600 diffractometer equipped with nickel filtration and Cu Kα radiation (λ = 1.5406 Å).

The XRD characterization results of the EFB ash-based K_2CO_3 catalyst showed diffraction patterns with sharp and clear peaks at various 2θ angles (Figure 1). The most dominant diffraction peak was detected at an angle of 2θ = 28.557° with a d-spacing of 3.123 Å. This peak has the highest intensity of 2353 cps and a narrow Full Width at Half Maximum (FWHM) of 0.174°, which indicates the presence of a crystalline phase with a high degree of structural regularity.

Based on calculations using the Scherrer equation, the main crystallite size of the catalyst was obtained to be approximately 47.2 nm, indicating that this material has nanocrystalline characteristics. The calculated lattice strain (ϵ) value of 1.1×10^{-3} indicates that the lattice distortion in the material is relatively small, indicating reasonable structural regularity and high phase stability. This suggests that the process of forming K_2CO_3 from EFB ash yields a catalyst with a regular crystal structure and potential for good catalytic activity.

In general, the low FWHM value on the prominent peaks, averaging <0.3°, is a strong indicator that this material has a high degree of crystallinity (Ali et al., 2022). The low FWHM value and large crystallite size are consistent with previous research findings, which report that the crystallite size of pure K_2CO_3 ranges from 40 to 50 nm (Houben et al., 2023; Masoud et al., 2022). These results indicate that the catalyst extracted from EFB ash has a crystallinity level equivalent to that of pure K_2CO_3. Therefore, the XRD results clearly confirm that the synthesized catalyst has a good crystalline structure, with no indication of a significant amorphous phase.

The diffraction peak detected at 2θ = 28.557° with a d-spacing of 3.123 Å has a perfect alignment with the typical diffraction pattern of K_2CO_3. Based on matching XRD data with JCPDS (Joint Committee on Powder Diffraction Standards) reference card number 9009644. The position of this peak is very consistent with the central peak present in crystalline K_2CO_3, which indicates that K_2CO_3 is the main compound in the EFB ash extract.

In addition, other significant peaks appeared at 2θ = 29.97°, 31.10°, 32.44°, 40.72°, 43.60°, 50.33°, 58.81°, 66.50°, and 73.79° with d-spacing values varying from 13.32 Å to 1.283 Å. All were successfully identified as the K_2CO_3 phase based

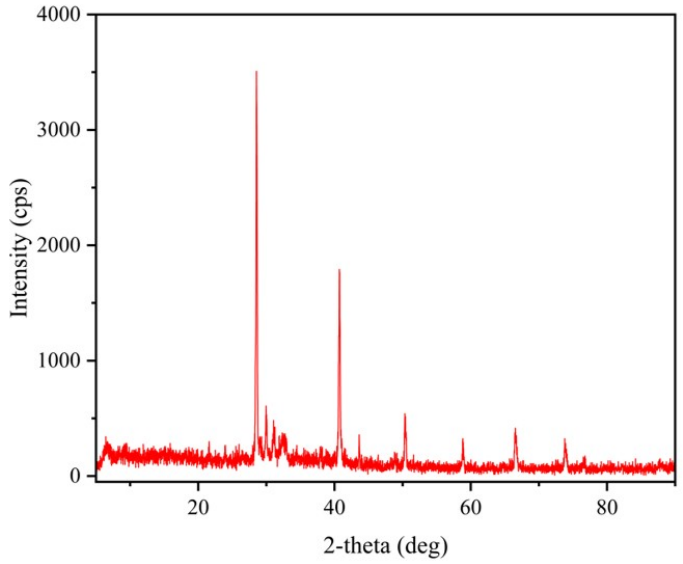

Figure 1. XRD Test Results of K_2CO_3 Catalyst

on matching with the JCPDS database card number 9009644. The presence of K_2CO_3 in the catalyst material comes from the natural content of the EFB ash. EFB ash is naturally known to have a high elemental potassium content, which is primarily present in the form of carbonate compounds, such as K_2CO_3. The presence of K_2CO_3 plays a crucial role in enhancing the alkaline nature of the material surface, which ultimately supports catalytic activity, particularly in transesterification reactions for biodiesel production. Strong alkaline properties can help in the activation process of methanol groups and accelerate the formation of methyl esters in the transesterification reaction (Kingkam et al., 2024).

The peak at the low angle of 2θ = 6.63°, which is relatively low in intensity, indicates the presence of layered structures or large interlayer spacing often found in mesoporous materials. This diffraction pattern exhibited by the EFB ash-based catalyst is typical of those found in biomass ash-based materials or solid catalysts. The crystalline phase provides more stable and organized active sites, which play a crucial role in maintaining catalyst efficiency during the reaction cycle (Dai and Zhang, 2021). The presence of a crystalline phase offers an advantage in catalytic applications, as it can enhance catalyst performance in chemical reactions.

3.1.2 SEM Analysis

Analysis of surface morphology and elemental composition of EFB ash-based K_2CO_3 catalyst was conducted using an SEM-EDX instrument. SEM (Scanning Electron Microscope) utilizes a focused electron beam to scan the surface of the sample, producing high-resolution images of the particles. The EDX (Energy-Dispersive X-ray Spectroscopy) detector, mounted on the SEM, is used to identify the elements in the catalyst based on the spectrum emitted by the atoms on the surface (Li et al., 2019). In this study, the SEM-EDX instrument (COXEM, Korea/(NeoScope^{TM} JCM-7000) and EDX detector (JEOL JED-2300) were used. The surface of the EFB ash-based K_2CO_3 catalyst analyzed using SEM is presented in Figure 2.

The characterization results obtained using a scanning electron microscope with a resolution of 5 μm for the EFB ash-based K_2CO_3 catalyst reveal that the catalyst exhibits an uneven, asymmetrical surface morphology and tends to form an aggregate structure. The catalyst surface appears to consist of lumps of irregularly shaped particles. Similar observations were reported by Arumugam and Sankaranarayanan (2020), who noted that the sugarcane leaf ash catalyst used in biodiesel production formed clumps. Irregular aggregation was also observed in the SEM results of moringa leaf ash catalyst used in biodiesel production (Aleman-Ramirez et al., 2021). This irregular morphology is typically caused by the processes of fragmentation, melting, and agglomeration, as well as other changes that occur during combustion, resulting in particle fragments of varying sizes and shapes (Riaza et al., 2020; Manzoor et al., 2023). Additionally, the material's surface exhibits numerous voids and scattered pores. The presence of voids and pores on the material's surface can positively contribute to an increase in specific surface area, thereby supporting catalyst performance in heterogeneous reaction applications (Wang et al., 2024).

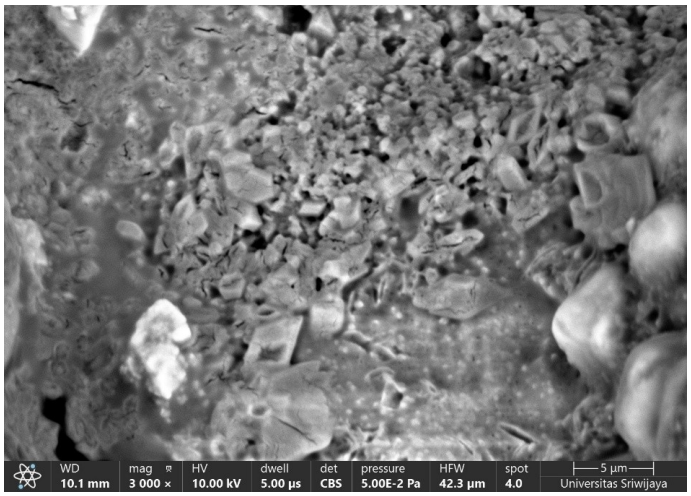

Figure 2. Surface EFB Ash-Based Catalyst

EDX analysis in this study aims to determine the chemical elements contained in the EFB ash-based catalyst. In the chemical composition test of the EFB ash-based K_2CO_3 catalyst used in this study, various components were detected, namely carbon (C), Oxygen (O), sodium (Na), silica (Si), phosphorus (P), sulfur (S), chloride (Cl), and Potassium (K). The desired target components are the elements potassium (K) and Oxygen (O), which form the K_2CO_3 compound. The results of the EDS analysis of the EFB ash-based K_2CO_3 catalyst are shown in Table 1.

The results of elemental composition analysis using EDX integrated with SEM observations (Table 1) show that the EFB

Table 1. EDX Analysis Results of EFB Ash-Based K_2CO_3 Catalyst

Elements	Atom (%)	Weight (%)	Signal Count
C	11.4	5.8	31 496
O	49.2	33.5	121 492
Na	0.7	0.7	5 203
Si	5.6	6.8	61 475
P	0.7	0.9	6 672
S	1.0	1.4	10 215
Cl	8.5	12.9	69 727
K	22.9	38.0	142 340

ash-based K_2CO_3 catalyst has an elemental composition dominated by Oxygen and Potassium. Oxygen was detected at 49.2% atoms, while Potassium reached 22.9% atoms or 38.0% by weight. The very high potassium content indicates that EFB ash is naturally rich in potassium-based compounds, particularly in the form of potassium carbonate, as confirmed previously through XRD analysis results. The presence of Potassium is significant because it functions as an active base center that contributes directly to catalytic activity by promoting the uptake of reactants (Peng et al., 2022).

In addition to these main elements, the element carbon was also detected at 11.4% atoms, most likely from the remaining organic material of the EFB that was not fully decomposed during the calcination process or was part of carbonate compounds such as K_2CO_3. The element silicon was detected at 5.6% atoms, indicating the presence of silica (SiO_2) as a natural inorganic component of the EFB ash. Silica acts as a supporting matrix, providing thermal and mechanical stability to the catalyst structure (Verma et al., 2020).

The presence of minor elements, such as sodium, phosphorus, sulfur, and chlorine, with contents ranging from 0.7% to 8.5% by atom, reflects the presence of natural mineral residues from the biomass. Sulfur and phosphorus, although in small amounts, have the potential to affect the chemical properties of the surface both as impurities and as modulators of active site activity. The high chlorine content (8.5% atoms or 12.9% by weight) indicates the presence of compounds such as potassium chloride (KCl) or sodium chloride (NaCl), which are common in palm biomass (Li et al., 2019; Babinszki et al., 2021).

The elemental composition rich in Potassium and Oxygen favors the formation of carbonate- and oxide-based structures that are strongly alkaline. This is in line with the morphological characteristics observed by SEM, where the catalyst surface appears irregular, porous, and forms particle aggregates of varying sizes. The presence of voids and pores on the material's surface provides a large specific surface area, increasing the number of active sites for catalytic reactions. The synergy between the active component K_2CO_3 and the inert component SiO_2 gives the catalyst an advantage in terms of both activity and structural stability.

The SEM-EDX spectrum image of the EFB ash-based K_2CO_3 catalyst (Figure 3) provides comprehensive information on the elemental composition of the catalyst surface. The spectrum exhibits high-intensity peaks in the energy ranges of approximately 0.5 keV for Oxygen and 3.3-3.6 keV for Potassium. The presence of these two elements in significant amounts indicates the dominance of oxide and carbonate compounds.

A carbon peak is identified at about 0.3 keV with moderate intensity, indicating the presence of residual carbon from biomass or part of carbonate compounds. Silicon exhibits a clear peak at around 1.74 keV, indicating the presence of the silica compound SiO_2, which serves as a support matrix. In addition, sodium, phosphorus, and sulfur are also present as minor components in the structure of the EFB ash and are detected at energies of about 1 keV, 2 keV, and 2.3 keV, respectively. The presence of chlorine is indicated by two distinct peaks at approximately 2.6 keV and 2.8 keV, with relatively high intensity. This indicates that the chlorine content is quite significant, which most likely originates from salt compounds such as potassium chloride or sodium chloride, naturally present in the EFB biomass.

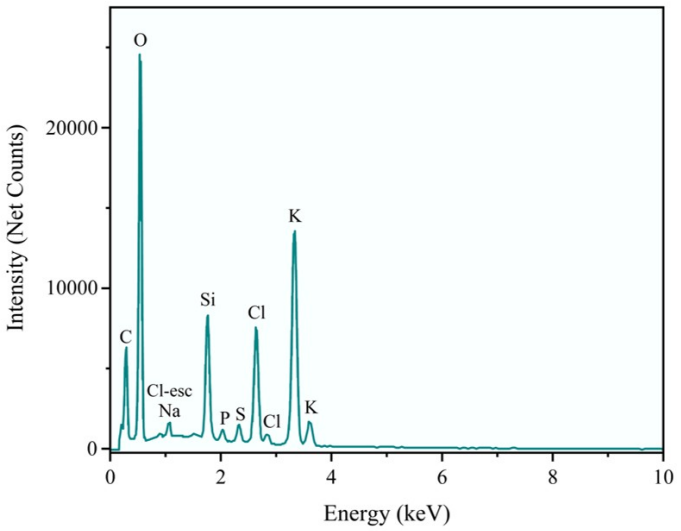

Figure 3. EDX Spectrum of EFB Ash-Based K_2CO_3

In general, the elemental distribution shown by the EDX spectrum is in line with the results of XRD analysis, which confirms the dominance of the K_2CO_3 phase in this EFB ash-based catalyst material. The EFB ash-based K_2CO_3 catalyst is rich in active base components, particularly K_2CO_3, which is crucial in catalytic transesterification reactions. The high potassium content is the leading indicator of the potential of this catalyst as a heterogeneous base catalyst. Additionally, the presence of inert components, such as silica and a small amount of other minerals, can help improve the structural stability of the catalyst.

3.1.3 XRF Analysis

The results of X-ray fluorescence (XRF) analysis (Table 2) show that the EFB ash-based K_2CO_3 catalyst contains dominant elements that are strong bases, with the main composition consisting of Potassium, calcium, phosphorus, and magnesium. The element potassium was detected in very high concentrations, reaching 41.604% in elemental form and 45.573% in the form of K_2O compounds. This potassium content confirms that EFB ash has powerful alkaline properties. The presence of K_2O is a key indicator of the material's ability to act as a heterogeneous base catalyst.

In addition to Potassium, the element calcium is also found in a significant amount, equivalent to 23.267% of the element, which is equivalent to CaO at 20.614%. Calcium oxide is also a potent base compound that is widely applied in heterogeneous catalysis. The presence of CaO not only strengthens the basic properties but also increases the thermal stability of the catalyst (Mazaheri, 2021). The phosphorus content is also extensive, namely 20.133% of the element, or P_2O_5, at 18.113%. Phosphorus is typically associated with phosphate compounds that can modify the surface properties of catalysts, affecting both base distribution and structural stability (Walkowiak et al., 2024). The high P_2O_5 content in the EFB ash is unique compared to other biomass ashes and may contribute to different or more complex catalytic activities. The high P_2O_5 content may provide additional advantages in active site modification or material stability (Garbarino et al., 2022).

The magnesium element was also found at 10.133% and MgO at 8.004%, which acts as a weak base and is often combined with potent base compounds to produce a more even distribution of base strength on the catalyst surface. The presence of MgO can also increase the catalyst's resistance to deactivation. Minor elements detected include sulfur at 1.811% (S) or SO_3 at 3.992%, iron at 1.49% (Fe) or Fe_2O_3 at 1.555% and other elements present in low concentrations, such as Cl, Ti, Mn, Cu, Zn, As, Rb, Sr, Zr, and Ba (<1%). Nonetheless, these elements may play a role in strengthening the material structure or indirectly affect the catalytic properties.

What is also quite striking is the non-detection of SiO_2 silica in these XRF results. Typically, biomass ash contains a substantial amount of silica, serving as an inert matrix. The absence of SiO_2 indicates that the characteristics of the EFB ash are different from other biomass ashes, with an absolute dominance of alkaline and alkaline earth-based compounds. Overall, the XRF results indicate that the EFB ash-based K_2CO_3 catalyst is a material rich in basic compounds, particularly K_2O and CaO, making it a strong candidate as a heterogeneous fundamental catalyst.

3.1.4 SAA Analysis

Textural characterization analysis was performed using the Brunauer–Emmett–Teller (BET) method through nitrogen (N_2) adsorption–desorption measurements at 77 K. The isothe rm curve obtained (Figure 4) shows an almost linear and flat pattern without apparent hysteresis, indicating a dense solid structure with low nitrogen adsorption capacity. Based on the IUPAC classification, this pattern corresponds to a type II isotherm, which generally describes non-porous to macroporous surfaces, where the adsorption process occurs on open and multilayer surfaces without the formation of capillarity in delicate pores (Thommes et al., 2015; Thommes and Cychosz, 2018; Rahman, 2021). The material lacks a developed microporous or mesoporous network. However, it does have macroporous voids or gaps between particles that are not significantly detected through (N_2) gas adsorption due to their size being much larger than that of nitrogen molecules (Thommes and Cychosz, 2018).

The textural parameter values obtained from BET and BJH analysis are summarized in Table 3. The results of multipoint BET analysis show a specific surface area of 0.11 m^2/g, a total pore volume of 1.8×10^{-4} cm^3/g, and an average pore radius of approximately 2 nm. The BET constant value (C = 19) and relatively low correlation coefficient (r = 0.65) indicate that the BET linear range is less than ideal, and the surface area obtained is close to the instrument detection limit. Nevertheless, these results provide important information that the active phase of K_2CO_3 or oxide is distributed on a compact solid surface. At the same time, the presence of macropores, as observed through SEM, continues to play a role in increasing the diffusion pathway for reactants and products during the catalytic reaction (Lukić et al., 2009).

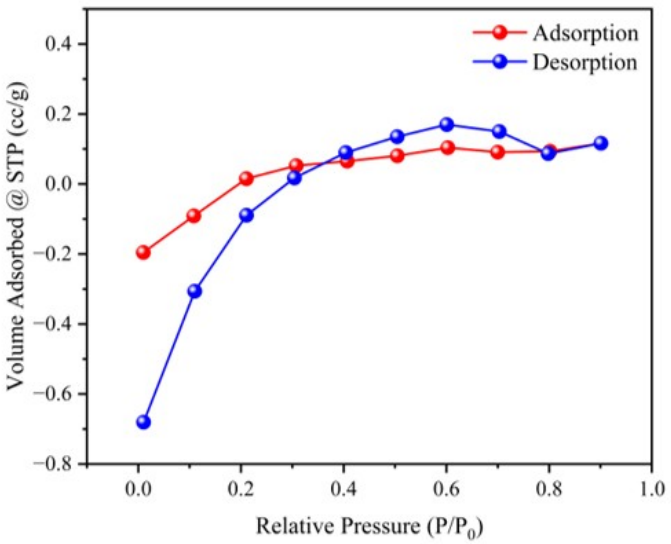

Figure 4. N_2 Adsorption–Desorption Isotherm at 77 K

Low textural characteristics do not always reduce catalytic performance. In many heterogeneous systems, reaction activity is determined more by surface chemical properties, metal-support bonds, and base site strength than by geometric surface area alone (Changmai et al., 2020). The presence of macroporous voids resulting from particle aggregation can facilitate the diffusion of reactants to active sites. At the same time, the compact structure offers good thermal stability and reduces

Table 2. XRF Test Result of EFB Ash-Based K_2CO_3 Catalyst

Element		Geology		Oxide	
Component	Level (%)	Component	Level (%)	Component	Level (%)
Na	0	Na_2O	0	Na_2O	0
Mg	10.133	MgO	8.09	MgO	8.004
Si	0	SiO_2	0	SiO_2	0
P	20.133	P_2O_5	18.098	P_2O_5	18.113
S	1.811	SO_3	3.996	SO_3	3.992
Cl	0.15	Cl	0.128	K_2O	45.573
K	41.604	K_2O	46.704	CaO	20.614
Ca	23.267	CaO	20.447	TiO_2	0.133
Ti	0.109	Ti	0.08	MnO	0.126
Mn	0.133	Mn	0.098	Fe_2O_3	1.555
Fe	1.49	Fe_2O_3	1.559	CuO	0.886
Cu	0.124	Cu	0.09	ZnO	0.243
Zn	0.147	Zn	0.107	As_2O_3	0.004
As	0.133	As	0.003	Rb_2O	0.24
Rb	0.302	Rb	0.26	SrO	0.188
Sr	0.219	Sr	0.16	Y_2O_3	0
Y	0	Y	0	ZrO_2	0.003
Zr	0.003	Zr	0.002	BaO	0.198
Ba	0.242	Ba	0.178	Eu_2O_3	0
Eu	0	Eu	0	Cl	0.128

the likelihood of sintering of the active particles. Thus, even though the specific surface area is relatively low, this EFB ash catalyst still has the potential to exhibit stable catalytic activity if the active sites are evenly distributed and have strong bonding strength to the support.

Overall, the characterization results indicate that the TKKS ash-based K_2CO_3 catalyst exhibits a regular crystalline structure, with a predominance of the intense base phase K_2CO_3/K_2O, as confirmed through XRD and XRF analysis. The irregular surface morphology and tendency to form solid aggregates, as observed in the SEM results, are in line with the findings of the BET analysis, which shows a type II isotherm with a low surface area but the presence of interparticle macroporous structures. This condition indicates that the active potassium phase has been effectively dispersed on a stable solid surface, rather than in a large porous structure. Although the surface area is small, the presence of strong base sites in the crystalline phase provides high catalytic activity potential and good thermal stability. These structural and surface chemical characteristics play a crucial role in facilitating mass transport during transesterification reactions.

3.2 Comparison of Characteristics of K_2CO_3 Catalyst based on EFB ash and Commercial K_2CO_3

To get a more comprehensive understanding, XRD, SEM-EDX, and XRF tests were also analyzed on commercial K_2CO_3 catalysts for comparison. The XRD test results of the commercial K_2CO_3 catalyst (Figure 5) show a sharper and more intense diffraction pattern. When compared to the EFB ash-based K_2CO_3 catalyst which has main 2θ XRD patterns at 28.55°, 29.96°, 31.10°, 32.44°, 40.71°, 43.60°, 50.32°, 58.81°, 66.49°, and 73.79°, the commercial K_2CO_3 catalyst has strong peaks at 29.76°, 32.68°, 32.39°, 38.60°, 39.15°, and 40.55°. The commercial K_2CO_3 catalyst also has a minimal FWHM value on the main peak, which is on average 0.13-0.25, indicating that commercial K_2CO_3 has a high level of crystallinity. The FWHM value is not significantly different when compared to the EFB ash-based K_2CO_3 catalyst, which has a FWHM of 0.17-0.3 K_2CO_3 exhibits high crystallinity but also displays the presence of minor amorphous phases or impurity minerals.

Table 3. Textural Parameters from BET, BJH, and t-Plot Analysis

Parameter	Value	Unit
Specific surface area (SBET)	0.11	m^2/g
BET constant (C)	19.3	–
Total pore volume	1.8×10^{-4}	cm^3/g
Average pore diameter	2.0	nm
BJH surface area (adsorption)	0.115	m^2/g
BJH pore volume (desorption)	2.96×10^{-4}	cm^3/g
Micropore volume	0.00	cm^3/g

SEM results of the surface of the commercial K_2CO_3 catalyst reveal more homogeneous particles, a smooth surface with a more regular shape, which reflects the level of purity and control achieved in the production process (Figure 6). Like the EFB ash-based K_2CO_3 catalyst, the composition of commer-

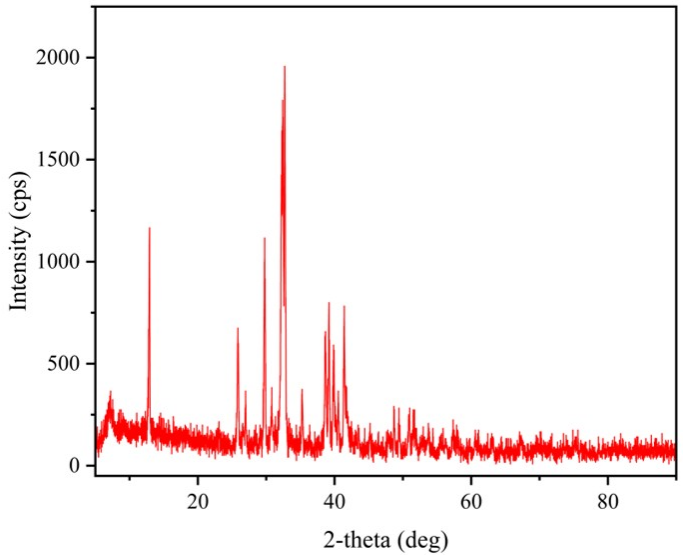

Figure 5. XRD Result of Commercial K_2CO_3 Catalyst

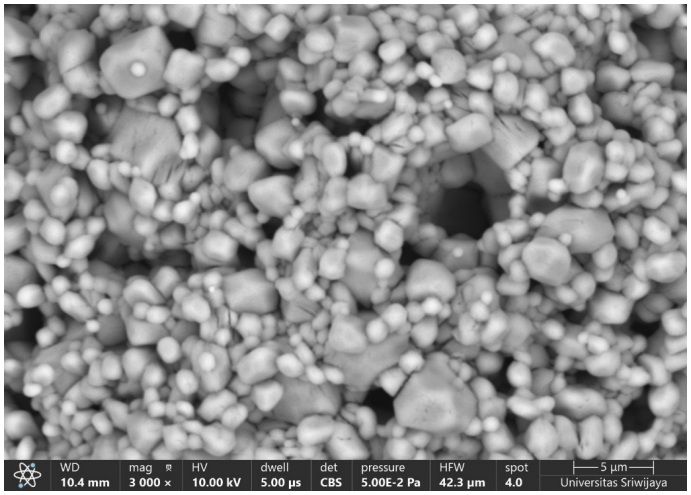

Figure 6. Surface of Commercial K_2CO_3 Catalyst

cial K_2CO_3 catalyst is also dominated by Potassium, Oxygen, and carbon elements with higher concentrations.

The EDX results (Table 4) indicate that the commercial K_2CO_3 is predominantly composed of oxygen (50.3% At.%) and potassium (34.0% At.%), with carbon content (15.7% At.) suggesting the possible presence of carbon residues from the catalyst manufacturing or processing stages.

Table 4. EDX Analysis Result of Commercial K_2CO_3 Catalyst

Element	Atom (%)	Weight (%)	Signal Number
C	15.7	8.1	94 148
O	50.3	34.7	102 724
K	34.0	57.2	198 889

The SEM-EDX spectrum (Figure 7) exhibits high intensity peaks at approximately 0.5 keV for oxygen and 3.3–3.6 keV for potassium, confirming the dominance of oxide and carbonate compounds. No other elements, such as silicon (Si), chlorine (Cl), sodium (Na), phosphorus (P), or sulfur (S), were detected. This indicates that the commercial K_2CO_3 has a high level of purity and is free from contaminants. In comparison, the K_2CO_3 catalyst derived from TKKS ash contains minor elements, including silicon, sodium, phosphorus, sulfur, and chlorine, detected at energy levels ranging from 1 to 2.8 keV. Thus, the commercial K_2CO_3 exhibits a purer composition.

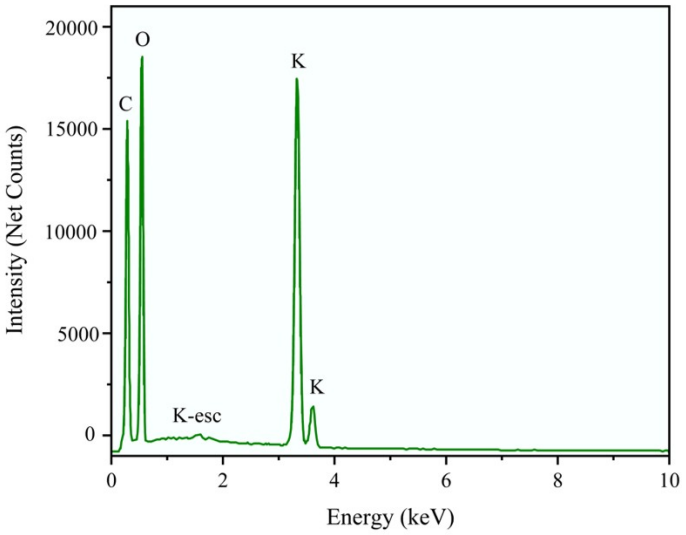

Figure 7. EDX Spectrum of Commercial K_2CO_3 Catalyst

The results of the XRF analysis show quite striking differences in chemical composition between K_2CO_3 obtained from EFB ash and commercial K_2CO_3 (Table 5). The potassium content in commercial K_2CO_3 reaches 80.721% or K_2O of 80.281%, reflecting a very high level of purity. In comparison, EFB ash-based K_2CO_3 has a potassium content of 41.604% or K_2O of 45.573%, but still shows significant potential as a source of potassium-based compounds. In addition, EFB ash-based K_2CO_3 contains higher calcium, namely 23.267% elemental or 20.614% CaO, while commercial K_2CO_3 is only 15.423% elemental or 15.686% CaO. This indicates the contribution of natural mineral residues that have the potential to enhance the basic properties, but at the same time indicate a lower level of purity. The high phosphorus content in the EFB ash-based K_2CO_3 catalyst is 20.133% elemental or 18.113% P_2O_5, but was not significantly detected in commercial K_2CO_3. In contrast, the silica content of SiO_2 was detected in commercial K_2CO_3 at 1.313% but not in EFB ash-based K_2CO_3. Minor elements such as Fe, Ti, Mn, Cu, Zn, and Sr were found in both commercial K_2CO_3 and EFB ash-based K_2CO_3 at relatively low concentrations (<2%), which are generally derived from biomass-derived minerals or remnants from the production process. Chloride was also at a higher concentration in commercial K_2CO_3 (0.252% elemental) compared to the EFB ash-

based K_2CO_3 (0.15% elemental). These results demonstrate that, although the EFB ash-based K_2CO_3 has a lower purity level than the commercial product, its chemical composition still makes it a promising candidate for catalytic applications, particularly in processes that require high alkaline properties.

3.3 Catalytic Performance in Biodiesel Production

The data in Table 6 shows the effect of catalyst weight variation on the yield of biodiesel production from RBDPO feedstock using methanol. The catalyst variation starts from 3 grams to 12 grams. The weight of the catalyst has a significant impact on the yield of glycerol and biodiesel. At a catalyst usage of 3 grams, the biodiesel obtained after evaporation amounted to 85.89 grams, with 17.64 grams of glycerol remaining. The biodiesel yield reached its highest number at a catalyst dose of 3 grams, indicating that at low catalyst doses, the transesterification reaction runs efficiently without the formation of excessive by-products. When the catalyst dose was increased to 6 grams, the biodiesel produced after evaporation dropped to 77.96 grams, and the amount of glycerol dropped to 15.75 grams. This phenomenon indicates that the excessive addition of catalyst promotes the saponification reaction, where the oil reacts with the basic catalyst to form soap, thus reducing the biodiesel yield.

The decrease in biodiesel yield was even more pronounced at catalyst weights of 9 grams and 12 grams, producing 75.96 grams and 72.14 grams of biodiesel, respectively. Directly proportional to the biodiesel yield, the amount of glycerol produced also decreased along with the increase in the amount of catalyst used. The use of 9 grams and 12 grams of catalyst produced 13.07 grams and 10.75 grams of glycerol, respectively. The production of biodiesel, which is inversely proportional to the amount of catalyst used, confirms that there is an optimum limit to the use of catalyst in the transesterification process. Excessive catalyst doses do not always yield better results; instead, they can harm biodiesel yield due to side reactions. Overall, the biodiesel production data using the powder catalyst indicated that the optimal condition for producing the highest biodiesel yield of 85.89% was achieved with 3 grams of catalyst.

The catalytic performance of this K_2CO_3/EFB catalyst is closely related to its structural characteristics, elemental composition, and surface texture. The XRD pattern shows sharp crystalline peaks associated with the K_2CO_3 and K_2O phases, indicating the presence of strong base sites (K^+–O^{-2}) that serve as the main active centers. The regular crystalline phase (crystallite size, 47.2 nm) and low lattice strain (1.1×10^{-3}) indicate good structural stability, supporting the formation of methoxide ions (CH_3O^-) during the reaction, which is a crucial initial step in the transesterification mechanism.

The SEM image reveals an irregular and aggregated surface morphology, characterized by several scattered cavities and small pores. This structure increases the oil–methanol–catalyst contact area and facilitates the diffusion of reactant molecules towards the active sites. SAA (BET) analysis indicates that the obtained N_2 adsorption-desorption isotherm belongs to type II according to the IUPAC classification, characterizing a non-porous to macroporous surface. This indicates that although there is no developed microporous or mesoporous network, the material still has macroporous voids or interparticle gaps that can play a role in mass transport.

The very low specific surface area (0.11 m^2/g) with a pore volume of 1.8×10^{-4} cm^3/g and a pore radius of approximately 2 nm indicates that most of the solid surface is dense. In contrast, large pores cannot be detected by nitrogen molecules due to the limitations of the BET method. This low surface area explains that catalytic activity does not primarily depend on geometric area, but rather on the strength and density of surface base sites originating from metal oxide compounds (K_2O, CaO). The presence of macropores, visible in the SEM results, also facilitates the diffusion of reactants and products, thereby supporting the effectiveness of interphase contact in the solid-liquid catalyst system.

In addition, the EDX results confirm the dominance of Potassium and Oxygen, indicating that K^+ ions act as the main base sites in the conversion of triglycerides to methyl esters. XRF data support this finding by showing a high potassium content (= 41.6%), followed by Ca, P, and Mg. The high K content indicates the dominance of a strong base phase (K_2O/K_2CO_3), while the presence of Ca and P contributes to the formation of medium to weak base sites (CaO, $Ca_3(PO_4)_2$). This combination forms a complementary hierarchy of active sites, where K^+ activates methanol into methoxide ions, while Ca^{2+} and P help stabilize the catalyst surface and accelerate the formation of methyl esters.

The catalytic activity of this catalyst is primarily attributed to the presence of metal oxide compounds containing K^+ and Ca^{2+} ions, which play a crucial role in the formation of methoxide ions during the transesterification reaction (Tsai and Tsai, 2024). The high potassium content in the extracted catalyst supports strong surface basicity and higher reaction efficiency, while the presence of Ca and P elements detected has the potential to contribute additionally as secondary active sites (Maj et al., 2025).

Based on XRF results, the detected potassium content was significantly higher than that of calcium, indicating the dominance of an intense basic phase (K_2O/K_2CO_3) over a moderate basic phase, such as CaO. This dominance is consistent with the high biodiesel yield (85.89%), as the presence of strong base sites plays an important role in the formation of methoxide ions that initiate the transesterification reaction. This finding is consistent with previous research reports, which show that catalytic activity in solid base systems is more controlled by base site strength and surface chemical composition than by total surface area (Mat, 2012; Changmai et al., 2020).

High catalytic activity is controlled by the density and streng th of surface base sites, not by the total geometric surface area. This finding is consistent with previous reports on biomass ash-based base catalysts, which show a direct relationship between alkali metal content and the transesterification rate (Ao et al., 2024). Thus, the combination of a stable crystalline structure,

Table 5. Comparison of XRF Test Results of EFB Ash-Based and Commercial K_2CO_3 Catalysts

Element			Geology			Oxide		
Component	K_2CO_3 EFB	Commercial K_2CO_3	Component	K_2CO_3 EFB	Commercial K_2CO_3	Component	K_2CO_3 EFB	Commercial K_2CO_3
Na	–	–	Na_2O	–	–	Na_2O	–	–
Mg	10.133	–	MgO	8.09	–	MgO	8.004	–
Si	–	1.195	SiO_2	–	1.313	SiO_2	–	1.311
P	20.133	–	P_2O_5	18.098	–	P_2O_5	18.113	–
S	1.811	–	SO_3	3.996	–	SO_3	3.992	–
Cl	0.15	0.252	Cl	0.128	0.217	K_2O	45.573	80.281
K	41.604	80.721	K_2O	46.704	80.393	CaO	20.614	15.686
Ca	23.267	15.423	CaO	20.447	15.743	TiO_2	0.133	0.213
Ti	0.109	0.173	Ti	0.08	0.128	MnO	0.126	0.151
Mn	0.133	0.158	Mn	0.098	0.117	Fe_2O_3	1.555	1.853
Fe	1.49	1.761	Fe_2O_3	1.559	1.857	CuO	0.886	0.138
Cu	0.124	0.15	Cu	0.09	0.11	ZnO	0.243	0.151
Zn	0.147	0.166	Zn	0.107	0.122	As_2O_3	0.004	0.216
As	0.133	–	As	0.003	–	Rb_2O	0.24	–
Rb	0.302	–	Rb	0.26	–	SrO	0.188	–
Sr	0.219	–	Sr	0.16	–	Y_2O_3	–	–
Y	–	–	Y	–	–	ZrO_2	0.003	–
Zr	0.003	–	Zr	0.002	–	BaO	0.198	–
Ba	0.242	–	Ba	0.178	–	Eu_2O_3	–	–
Eu	–	–	Eu	–	–	Cl	0.128	–

Table 6. Measurement Data and Biodiesel Yield (Powder Catalyst)

Catalyst weight (g)	Methanol (g)	RBDPO (g)	Gliserol (g)	Biodiesel (g)	Yield (%)
3			17.92	85.89	85.89
6			17.64	77.96	77.96
9	30	100	15.75	75.96	75.96
12			11.04	72.14	72.14

All data are averages from three repetitions of the experiment (n = 3)

the presence of interparticle macroporous cavities, and the dominance of strong K^+-O^{2-} base sites forms a synergy that supports high catalytic activity despite the low surface area.

The transesterification reaction mechanism on the K_2CO_3/EFB catalyst can be explained as a process catalyzed by a heterogeneous base, in which surface base sites-including the K_2O phase and K^+-O^{2-} site pairs-abstract protons from methanol to form methoxide ions (CH_3O^-). It is this methoxide ion that then attacks the carbonyl group in triglycerides, producing methyl esters and glycerol as by-products (Trejo-Zárraga et al., 2018). On the other hand, Ca^{2+} ions act as Lewis acid sites, polarizing the carbonyl group and thereby accelerating the nucleophilic attack by methoxide ions. Phosphorus (P) plays a role in stabilizing the K^+ active site and preventing its deactivation during the reaction.

The decrease in biodiesel yield at higher catalyst doses is most likely caused by soap formation (saponification) due to excess base sites, which reduces the availability of methoxide for the main transesterification pathway and interferes with phase separation (Pecha et al., 2016). This condition is reinforced by SAA results, which show the dominance of non-porous to macroporous solid structures. In these structures, solid surfaces tend to saturate quickly at high catalyst concentrations, thereby reducing interphase contact efficiency.

It should be noted that reuse and regeneration tests were not performed in this study because the amount of catalyst remaining after the transesterification reaction was relatively small. Most of the fine powder catalyst adhered to the reactor walls during the reaction process, making it difficult to recover completely, which is a common disadvantage of using powdered heterogeneous catalysts. In addition, some of the catalyst was also dissolved in the filtrate and lost during the separation stage due to its easily dispersible nature. This condition results in an insufficient amount of catalyst remaining to perform a reliable regeneration test. Therefore, further research will focus on developing K_2CO_3/EFB catalyst pellets, which are ex-

pected to minimize catalyst loss during the process and enable systematic evaluation of stability and regeneration.

These results also confirm that catalysts extracted from EFB ash have good catalytic activity in transesterification reactions. As a comparison, several previous studies have reported the catalytic activity of untreated biomass ash and pure K_2CO_3. The use of 2% pure K_2CO_3 was able to produce a biodiesel yield of around 94–98% under similar conditions (Salam et al., 2024), while raw EFB ash also showed high catalytic activity with a yield of 96–98% (Komariah et al., 2024).

Although this study did not conduct direct control experiments using untreated EFB ash or pure K_2CO_3, the results obtained can still be interpreted with reference to those studies. The slightly lower biodiesel yield (85.89%) indicates that the EFB extraction catalyst still exhibits good catalytic activity, despite being influenced by factors such as potassium ion content, binding, surface alkalinity, and structural changes. The extraction process is thought to cause redistribution of some of the active base phases, thereby affecting the availability of K active sites compared to pure or untreated catalysts. However, this modification may also provide better thermal and structural stability during the reaction. Nevertheless, the use of EFB extraction catalyst provides significant added value because it utilizes agricultural waste to create an environmentally friendly and sustainable heterogeneous catalyst, thereby reducing dependence on pure chemicals.

3.4 Characteristics of Biodiesel Produced

The chemical composition and FAME fraction of the biodiesel were characterized using the GC-MS technique. GC-MS spectra provide a thorough understanding of biodiesel quality and standards. The GC-MS spectrum showed significant peaks of the biodiesel under the use of palm empty fruit bunch-based K_2CO_3 catalyst (Figure 8). The peaks were validated using software that utilized library reference data. Methyl esters of hexadecanoic acid, 9-octadecanoic acid, dodecanoic acid, methyl tetradecanoate, and methyl stearate were among the FAME peaks found. These peaks are in agreement with previous studies conducted on the synthesis of FAME from seed oil, which showed similar peaks of Octadedecadienoic (Z, Z)-acid, methyl ester, Decanoic acid, methyl ester, Dodecanoic acid, methyl ester and Hexcadecanoic acid, methyl ester (Kanwal et al., 2025; Munir, 2025; Rozina et al., 2025).

Analysis of the fatty acid methyl ester (FAME) compound profile shows that the form and concentration of the EFB ash-based K_2CO_3 catalyst have a significant effect on the composition of the fatty acids formed. Table 6 presents the relative abundance of each fatty acid formed. The main compounds identified include palmitic acid, oleic acid, stearic acid, linoleic acid, lauric acid, and myristic acid. Palmitic acid, as one of the dominant components in palm oil-based biodiesel, exhibited a high abundance and was relatively stable across various catalyst concentrations. The abundance of palmitic acid ranged from 29 to 32%. The stability of this saturated acid formation indicates that the transesterification process of the palmitic acid precursor is not significantly influenced by the catalyst dosage used.

In contrast, oleic acid was the dominant component in the reaction using powder catalysts and experienced significant fluctuations, especially in the pellet catalyst. The abundance of oleic acid in the powder catalyst was relatively stable, ranging from 41% to 50%. Meanwhile, stearic acid and lauric acid exhibited relatively small and insignificant fluctuations in all treatments. The relative abundance of stearic acid and lauric acid ranged from 6 to 8%, indicating that the formation of stearic acid is quite resistant to variations in reaction conditions, as determined by catalyst concentration.

Table 7. Fatty Acid Profile of Biodiesel

Common Name	3%	6%	9%	12%
Palmitic Acid	30	30	29	31
Oleic Acid	41	50	42	43
Stearic Acid	8	-	8	7
Lauric Acid	6	6	6	-
Myristic Acid	15	14	15	17

3.5 Evaluation of Sustainability and Techno-economics of K_2CO_3 Catalyst Based on Palm Oil Empty Bunch Ash

In line with the principles of green chemistry and the concept of waste valorization, the use of K_2CO_3 catalysts synthesized from oil palm empty fruit bunches (EFB) ash shows significant potential in supporting the sustainability of biodiesel production and environmental protection. EFB is a lignocellulosic biomass waste that is abundant (approximately 23% of every ton of fresh fruit bunches processed) and is often underutilized (Santi et al., 2019). Converting this waste into functional catalysts not only reduces the environmental impact caused by open burning or disposal in landfills, but also adds value to the waste (Trejo-Zárraga et al., 2018; Tsai and Tsai, 2024). By converting this waste into an active catalyst, this approach aligns with the principles of green chemistry and the circular economy, while also mitigating the environmental impacts associated with conventional solid waste disposal (Sai Bharadwaj et al., 2025).

From an environmental perspective, the use of EFB ash as a catalyst offers major advantages because it avoids the use of synthetic chemicals and leverages renewable local resources. The catalyst production process is carried out at relatively low temperatures with simple steps, thereby minimizing energy consumption and greenhouse gas emissions (Babinszki et al., 2021). Unlike conventional homogeneous catalysts such as NaOH and KOH, which require complex post-reaction purification processes and generate large amounts of liquid waste (Changmai et al., 2020), heterogeneous catalysts derived from EFB ash allow for easier separation from the reaction mixture (Kibar et al., 2023). This significantly reduces liquid waste and lowers post-reaction processing costs. Moreover, this catalyst has the potential for reuse across multiple transesterification

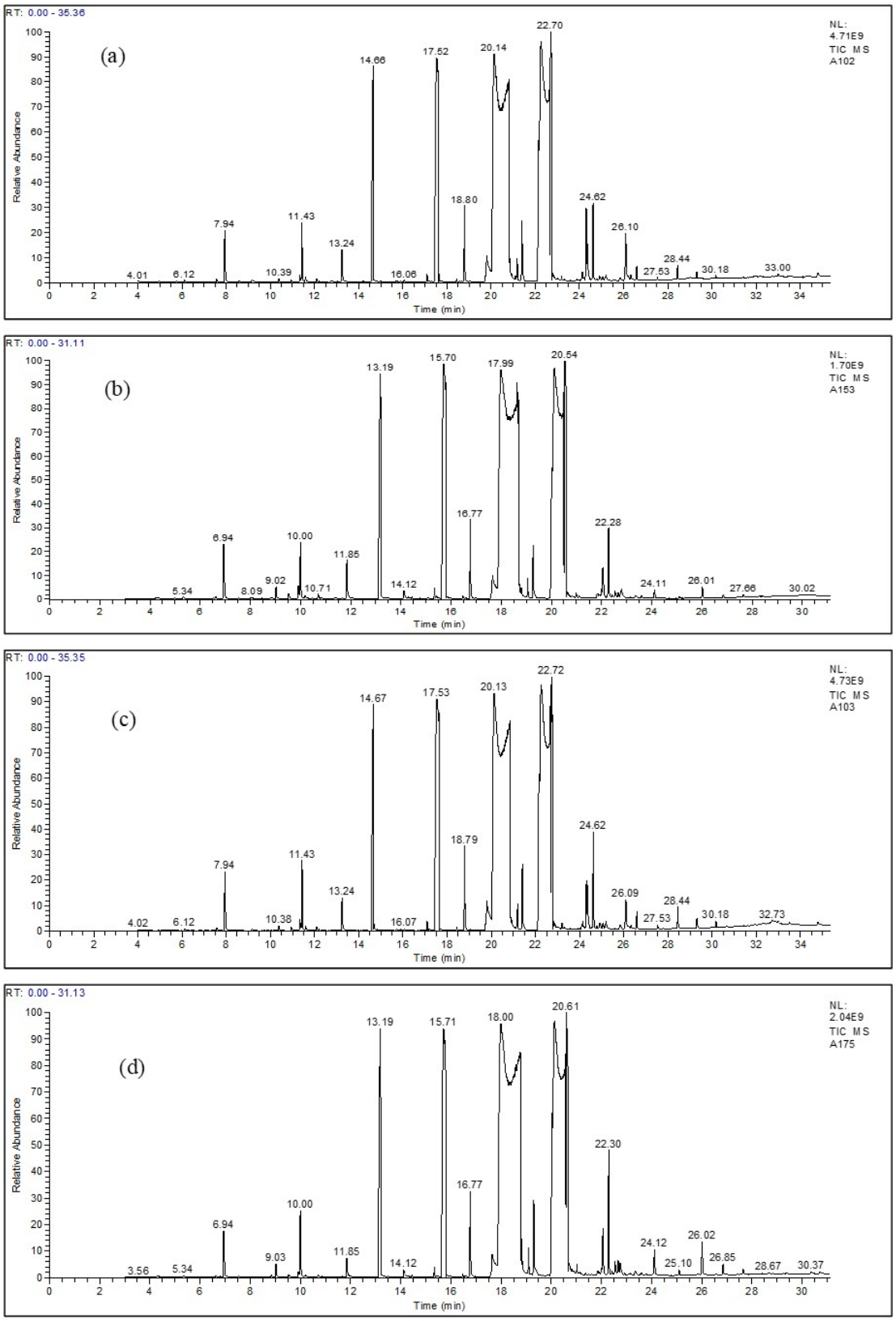

Figure 8. GC-MS Results of Biodiesel Powder Catalyst 3 g (a), 6 g (b), 9 g (c), 12 g (d)

cycles (Komariah et al., 2024). From a life cycle perspective, this approach supports the circular economy by reintegrating palm oil waste into the biodiesel production value chain (Lee et al., 2020).

From an economic standpoint, EFB ash, as a raw material, is highly available and very inexpensive, particularly in palm oil industry centers. The low cost of catalyst raw materials is crucial in enhancing the efficiency and competitiveness of biodiesel production. Environmentally friendly catalysts derived from biomass waste demonstrate economic viability with faster payback periods compared to acid and alkali catalysts (Gowthama Krishnan et al., 2024; Subramani et al., 2025). The efficient activation process, which does not require complex infrastructure, makes this technology economically feasible for medium to large-scale operations (Esmaeili, 2022). The high catalytic activity, with conversion rates reaching 85%, positions this catalyst as a competitive alternative to expensive conventional catalysts. Integrating this process within palm oil mills could reduce logistics costs and support integrated waste management.

Furthermore, this approach is not only relevant from a technical and economic standpoint but also provides positive social impacts. The utilization of local waste for renewable energy production opens opportunities for community empowerment, particularly in rural areas (Santhappan et al., 2025). Activities such as local catalyst production, technical training, and the development of micro-enterprises based on energy can drive inclusive and sustainable economic growth. In addition to supporting the diversification of downstream palm oil industry products, this strategy also contributes to achieving the Sustainable Development Goals (SDGs), particularly SDG 7 (Affordable and Clean Energy), SDG 12 (Responsible Consumption and Production), and SDG 13 (Climate Action). This approach also has the potential to improve the image of the palm oil industry, which has long been criticized for its environmental impacts (Hariyanti et al., 2024). Thus, the development and implementation of K_2CO_3 catalysts derived from EFB ash not only offer an efficient technological solution for biodiesel production but also demonstrate tangible potential in strengthening the environmental, economic, and social dimensions of sustainability in a holistic manner (Munasinghe, 2019; Sakai et al., 2022).

4. CONCLUSIONS

This study proved that EFB ash can be effectively used as a source of K_2CO_3 catalyst in biodiesel production through the transesterification reaction. Catalyst characterization revealed that the material possesses a good crystalline structure, high potassium content, and an irregular morphology with solid aggregates and macroporous interparticle voids, which support its catalytic activity. The results of BET-BJH-based Surface Area Analysis indicate a type II isotherm with a low specific surface area (0.11 m^2/g) and minimal pore volume, suggesting that catalytic activity is more influenced by the strength and distribution of base sites than by geometric surface area. Reactivity tests demonstrated that the K_2CO_3 catalyst derived from EFB ash can produce biodiesel with a high yield, reaching 85.89% at an optimum dose of 3 grams. In terms of sustainability, the use of EFB ash as a catalyst feedstock supports the reduction of biomass waste, lowers production costs, and mitigates emissions and environmental impacts associated with conventional biodiesel processes. The techno-economic evaluation indicates that the catalyst is cost-effective and suitable for industrial-scale applications, particularly in oil palm-producing regions. Therefore, the EFB waste-based K_2CO_3 catalyst has great potential as an eco-friendly and economical alternative heterogeneous catalysts to replace commercial catalysts in sustainable biodiesel production.

5. ACKNOWLEDGMENT

We want to express our gratitude to the Directorate of Research and Community Service, Directorate General of Research and Development, Ministry of Higher Education, Science and Technology of The Republic Indonesia, in accordance with the Implementation Contract of the State University Operational Assistance Program for Research Program Number: 109/C3/DT.05.00/PL/2025, which made this study possible. The financial support and resources have significantly contributed to the successful completion of this research. Special thanks also go to Universitas Sriwijaya, particularly the Energy Engineering and Waste Processing Laboratory, for their valuable support, resources, and collaboration throughout this research.

REFERENCES

Ahmad, W., J. Nisar, F. Anwar, and F. Muhammad (2023). Future Prospects of Biomass Waste as Renewable Source of Energy in Pakistan: A Mini Review. *Bioresource Technology Reports*, **24**; 101658

Aleman-Ramirez, J. L., J. Moreira, S. Torres-Arellano, A. Longoria, P. U. Okoye, and P. J. Sebastian (2021). Preparation of a Heterogeneous Catalyst from Moringa Leaves as a Sustainable Precursor for Biodiesel Production. *Fuel*, **284**; 118983

Ali, A., Y.-W. Chiang, and R. M. Santos (2022). X-Ray Diffraction Techniques for Mineral Characterization: A Review for Engineers of the Fundamentals, Applications, and Research Directions. *Minerals*, **12**(2); 205

Ao, S., J. Kim, S. Lee, J. Park, and H. Kim (2023). Microwave-Assisted Sustainable Production of Biodiesel: A Comprehensive Review. *Current Microwave Chemistry*, **10**(1); 3–25

Ao, S., J.-W. Kim, S. Lee, J. Park, H. Kim, M. Choi, and D. Lee (2024). Biomass Waste-Derived Catalysts for Biodiesel Production: Recent Advances and Key Challenges. *Renewable Energy*, **223**; 120031

Arumugam, A. and P. Sankaranarayanan (2020). Biodiesel Production and Parameter Optimization: An Approach to Utilize Residual Ash from Sugarcane Leaf, a Novel Heterogeneous Catalyst, from Calophyllum Inophyllum Oil. *Renewable Energy*, **153**; 1272–1282

Atadashi, I. M., M. K. Aroua, and A. A. Aziz (2011). Biodiesel Separation and Purification: A Review. *Renewable Energy*, **36**(2); 437–443

Athar, M. and S. Zaidi (2020). A Review of the Feedstocks, Catalysts, and Intensification Techniques for Sustainable Biodiesel Production. *Journal of Environmental Chemical Engineering*, **8**(6); 104523

Awosusi, A. A., A. Ibrahim, J. Abdulkareem, E. James, A. Usman, C. Michael, and J. Bello (2022). The Dynamic Impact of Biomass and Natural Resources on Ecological Footprint in BRICS Economies: A Quantile Regression Evidence. *Energy Reports*, **8**; 1979–1994

Babinszki, B., T. Kéri, G. Szabó, B. Székely, A. Molnár, and Z. Varga (2021). Thermal Decomposition of Biomass Wastes Derived from Palm Oil Production. *Journal of Analytical and Applied Pyrolysis*, **155**; 105069

Balajii, M., S. Niju, R. Karthikeyan, S. Ramu, R. Dhanasekaran, and B. Muthukumar (2019). A Novel Biobased Heterogeneous Catalyst Derived from *Musa acuminata peduncle* for Biodiesel Production – Process Optimization Using Central Composite Design. *Energy Conversion and Management*, **189**; 118–131

Basumatary, S. F., B. Das, P. Kalita, S. L. Rokhum, S. Basumatary, M. Dutta, and A. Hazarika (2023). Advances in CaO-Based Catalysts for Sustainable Biodiesel Synthesis. *Green Energy and Resources*, **1**(3); 100032

Bhatia, S. K., Y. Sharma, P. S. Gill, H. Kaur, R. Singh, and A. Kumar (2020). Conversion of Waste Cooking Oil into Biodiesel Using Heterogeneous Catalyst Derived from Cork Biochar. *Bioresource Technology*, **302**; 122872

Bo, F., C. Li, W. Zhang, J. Liu, X. Zhao, L. Wang, Y. Chen, and T. Huang (2025). Recent Advances in the Application of In Situ X-Ray Diffraction Techniques to Characterize Phase Transitions in Fischer–Tropsch Synthesis Catalysts. *Green Carbon*, **3**(1); 22–35

Buchori, L., A. Putra, H. Wibowo, A. Suryanto, P. Sanjaya, B. Nugroho, and B. Prasetya (2024). Preparation of KI/KIO3/Methoxide Kaolin Catalyst and Performance Test of Catalysis in Biodiesel Production. *Science and Technology Indonesia*, **9**(2); 359–370

Changmai, B., C. Vanlalveni, A. P. Ingle, R. Bhagat, and S. L. Rokhum (2020). Widely Used Catalysts in Biodiesel Production: A Review. *RSC Advances*, **10**(68); 41625–41679

Dai, J. and H. Zhang (2021). Recent Advances in Catalytic Confinement Effect within Micro/Meso-Porous Crystalline Materials. *Small*, **17**(22); 2005334

Esmaeili, H. (2022). A Critical Review on the Economic Aspects and Life Cycle Assessment of Biodiesel Production Using Heterogeneous Nanocatalysts. *Fuel Processing Technology*, **230**; 107224

Garbarino, G., G. Pampararo, E. Finocchio, G. Busca, A. Gervasini, S. Campisi, B. Silvestri, C. Imparato, and A. Aronne (2022). Surface Acid Properties of Nb_2O_5–P_2O_5–SiO_2 Gel-Derived Catalysts. *Microporous and Mesoporous Materials*, **343**; 112190

Garg, R., R. Sabouni, and M. Ahmadipour (2023). From Waste to Fuel: Challenging Aspects in Sustainable Biodiesel Production from Lignocellulosic Biomass Feedstocks and Role of Metal Organic Framework as Innovative Heterogeneous Catalysts. *Industrial Crops and Products*, **206**; 117554

Gowthama Krishnan, M., S. Rajkumar, and T. Devasagar (2024). The Sustainable Prospect of Biodiesel Production: Transformative Technologies, Catalysts from Bio-Wastes, and Techno-Economic Assessment. *Materials Today: Proceedings*

Hariyanti, F., P. Prasetyo, B. Nugroho, H. Wibowo, A. Suryanto, and L. Buchori (2024). Economic Transformation Based on Leading Commodities Through Sustainable Development of the Oil Palm Industry. *Heliyon*, **10**(4); e25674

Hazrat, M. A., M. G. Rasul, M. I. Jahirul, and M. A. Sattar (2024). Homogenous Alkaline Catalyst-Based Transesterification Process for Biodiesel Production From Sunflower Oil: Optimization and Kinetic Model Development. In *Biofuels: Green Fuels and Bioenergy*. Elsevier, pages 919–938

Houben, J., A. Shkatulov, H. Huinink, H. R. Fischer, and O. C. Adan (2023). Caesium Doping Accelerates the Hydration Rate of Potassium Carbonate in Thermal Energy Storage. *Solar Energy Materials and Solar Cells*, **251**; 112116

Ibrahim, N. A., U. Rashid, Y. H. Taufiq-Yap, T. C. S. Yaw, and I. Ismail (2019). Synthesis of Carbonaceous Solid Acid Magnetic Catalyst from Empty Fruit Bunch for Esterification of Palm Fatty Acid Distillate (PFAD). *Energy Conversion and Management*, **195**; 480–491

Ismaeel, H. K., T. Albayati, H. Dhahad, F. Al-Sudani, I. Salih, N. Saady, and S. Zendehboudi (2024). Strategies for Biodiesel Production With the Role of Reactor Technologies: A Comprehensive Review. *Chemical Engineering and Processing – Process Intensification*, **200**; 109767

Kanwal, S., Z. Ahmed, M. Khan, and et al. (2025). Elucidating the Potential of Non-Edible Milkweed Seed Oil for Biodiesel Production Using Green Pod-Derived Nano-Catalysts. *Waste Management Bulletin*, **3**(1); 27–38

Karmakar, B., S. L. Rokhum, and G. Halder (2022). Injecting Superheated C1 and C3 Alcohol Supports towards Non-Catalytic Semi-Continuous Conversion of Hevea Brasiliensis Oil into Biodiesel. *Fuel*, **314**; 122777

Khan, M. Z. A., F. A. Al-Sulaiman, S. U. Rehman, E. E. Ebenso, F. S. Mjalli, and I. S. Metcalfe (2023). Potential of Clean Liquid Fuels in Decarbonizing Transportation – An Overlooked Net-Zero Pathway? *Renewable and Sustainable Energy Reviews*, **183**; 113483

Kibar, M. E., B. Kibar, G. Seckin, A. Tekin, and K. Kara (2023). Assessment of Homogeneous and Heterogeneous Catalysts in Transesterification Reaction: A Mini Review. *ChemBioEng Reviews*, **10**(4); 412–422

Kingkam, W., W. Srifa, V. Puangpetch, P. Hengprakhon, C. Kongkaew, M. Sriariyanun, P. Pakdeeto, and S. Karnjanakom (2024). Synergistic Effect of La_2O_3–Al_2O_3 Based Catalysts for Efficient Biodiesel Production. *Journal of Indus-*

trial and Engineering Chemistry, **143**; 1–12
Komariah, L. N., S. Arita, and R. A. D. P. Ananda (2024). Effectiveness of Empty Fruit Bunch Ash as the Catalyst for Palm Oil Transesterification. *South African Journal of Chemical Engineering*, **50**; 65–74
Laskar, I. B., K. Rajkumari, R. Gupta, S. Chatterjee, B. Paul, and S. L. Rokhum (2018). Waste Snail Shell Derived Heterogeneous Catalyst for Biodiesel Production by the Transesterification of Soybean Oil. *RSC Advances*, **8**(36); 20131–20142
Lee, J.-C., H.-Y. Sun, S.-Y. Lee, Y.-H. Chou, and S.-H. Chang (2020). Preliminary Techno-Economic Analysis of Biodiesel Production over Solid-Biochar. *Bioresource Technology*, **306**; 123086
Li, M., P. Li, W. Zhang, C. Wang, Z. Liu, G. Liang, Y. Wu, Y. Ma, and X. Chen (2019). Effect of Residual Chlorine on the Catalytic Performance of Co_3O_4 for CO Oxidation. *ACS Catalysis*, **9**(12); 11676–11684
Lukić, I., G. van de Steene, J. van Haesendonck, J. J. Apperloo, and J. A. Martens (2009). Alumina/Silica Supported K_2CO_3 as a Catalyst for Biodiesel Synthesis from Sunflower Oil. *Bioresource Technology*, **100**(20); 4690–4696
Maj, I., K. Niesporek, P. Płaza, J. Maier, and P. Łoj (2025). Biomass Ash: A Review of Chemical Compositions and Management Trends. *Sustainability*, **17**(11); 4925
Manzoor, S., J. Tatum, O. B. Wani, and E. R. Bobicki (2023). Comminution of Carbon Particles in a Fluidized Bed Reactor: A Review. *Minerals Engineering*, **195**; 108026
Masoud, N., V. Clement, T. van Haasterecht, M. Führer, J. P. Hofmann, and J. H. Bitter (2022). Shedding Light on Solid Sorbents: Evaluation of Supported Potassium Carbonate Particle Size and Its Effect on CO_2 Capture from Air. *Industrial & Engineering Chemistry Research*, **61**(38); 14211–14221
Mat, R. (2012). Solid Catalysts and Their Application in Biodiesel Production. *Bulletin of Chemical Reaction Engineering & Catalysis*, **7**(2); 142–149.
Mazaheri, H. (2021). An Overview of Biodiesel Production via Calcium Oxide Based Catalysts: Current State and Perspective. *Energies*, **14**(13); 3950
Mohammed, A. S. (2023). A Comprehensive Review on the Effect of Ethers, Antioxidants, and Cetane Improver Additives on Biodiesel-Diesel Blend in CI Engine Performance and Emission Characteristics. *Journal of the Energy Institute*, **108**; 101227
Moreira, B. R. d. A. (2023). Biomass Off-Gassing: A Mini-Review and Meta-Analysis Aspiring to Inspire Future Research and Innovation in Solid Biofuels for Safety-Sensitive and Environmentally Responsible Residential and Industrial Applications. *Industrial Crops and Products*, **205**; 117508
Munasinghe, M. (2019). Value–Supply Chain Analysis (VSCA) of Crude Palm Oil Production in Brazil, Focusing on Economic, Environmental and Social Sustainability. *Sustainable Production and Consumption*, **17**; 161–175
Munir, M. (2025). Sustainable Biodiesel from Pyrus Pashia Seed Oil Using Sauromatum Venosum-Derived CdO Nanoparticles. *Sustainable Energy Technologies and Assessments*, **80**; 104372
Pecha, J., L. Šánek, T. Fürst, and K. Kolomazník (2016). A Kinetics Study of the Simultaneous Methanolysis and Hydrolysis of Triglycerides. *Chemical Engineering Journal*, **288**; 680–688
Peng, S.-S., X.-B. Shao, M.-X. Gu, G.-S. Zhang, C. Gu, Y. Nian, Y. Jia, Y. Han, X.-Q. Liu, and L.-B. Sun (2022). Catalytically Stable Potassium Single-Atom Solid Superbases. *Angewandte Chemie International Edition*, **61**(52); e202215157
Rahman, A., S. M. W. Murad, A. K. M. Mohsin, and X. Wang (2024). Does Renewable Energy Proactively Contribute to Mitigating Carbon Emissions in Major Fossil Fuels Consuming Countries? *Journal of Cleaner Production*, **452**; 142113
Rahman, M. (2021). Study on Optimum IUPAC Adsorption Isotherm Models Employing Sensitivity of Parameters for Rigorous Adsorption System Performance Evaluation. *Energies*, **14**; 7478
Reddy, K. V. (2023). Biomass Waste and Feedstock as a Source of Renewable Energy. In *Green Approaches to Alternative Fuels for a Sustainable Future*. Elsevier, pages 325–334
Riaza, J., P. E. Mason, J. M. Jones, A. Williams, J. Gibbins, and H. Chalmers (2020). Shape and Size Transformations of Biomass Particles During Combustion. *Fuel*, **261**; 116334
Rozina, O. E., M. Ahmad, A. Duduyemi, S. Ahmad, A. Khan, R. Esiaba, and C. Elekwachi (2025). Valorization of Waste Seed Oil from *Cupressus macrocarpa L.* for Biodiesel Production via Green-Synthesized Iron Oxide Nanoparticles: A Sustainable Approach toward Decarbonization. *Next Energy*, **7**; 100218
Sai Bharadwaj, A. V. S. L., R. R. Nayak, J. Koteswararao, C. Sampath, B. Gaddala, B. G. Pawar, and N. K. Gupta (2025). Environmental Life-Cycle Assessment and Green Principles in Process Intensification: A Review of Novel Catalysts from Solid Waste. *Chemical Engineering and Processing: Process Intensification*, **211**; 110208
Sakai, K., Y. Yamada, K. Takahashi, H. Suzuki, and A. Nakamura (2022). Promotion of a Green Economy with the Palm Oil Industry for Biodiversity Conservation: A Touchstone toward a Sustainable Bioindustry. *Journal of Bioscience and Bioengineering*, **133**(5); 414–424
Salam, Y. A., H. A. Nugroho, D. P. Putra, and R. I. Budiman (2024). Kinetics of Homogeneous Reaction of Potassium Methoxide Based on K_2CO_3 Catalyst in Transesterification of RBDPO to Biodiesel. *Science and Technology Indonesia*, **9**(1); 28–35
Santhappan, J. S., K. Narasimman, B. W. Winsly, A. F. Varghese, and T. Mathimani (2025). A Critical Evaluation of the Progression in Industrial Waste Utilization to Achieve Energy Transition Targets: Technological Obstacles, Carbon Footprint Reduction, and Life Cycle Assessment. *Renewable Energy*, **252**; 123469
Santi, L. P., D. N. Kalbuadi, and D. H. Goenadi (2019). Empty Fruit Bunches as Potential Source for Biosilica Fertilizer for

Oil Palm. *Journal of Tropical Biodiversity and Biotechnology*, **4**(3); 90–96

Subramani, S., R. Sambath, A. Ponnuvel, D. Kumaran, S. Rajesh, A. Murugesan, S. Muruhan, R. Sankar, D. M. Ganesan, and A. Arumugam (2025). Pilot Scale Production of Biodiesel from *Madhuca indica* and Comparative Techno-Economic Analysis. *Environmental Science and Pollution Research*

Sulaiman, N. F., M. F. Mat Tahar, N. Alherz, N. A. Ismail, H. H. Masjuki, and H. C. Ong (2020). Biodiesel Production from Refined Used Cooking Oil Using Co-Metal Oxide Catalyzed Transesterification. *Renewable Energy*, **153**; 1–11

Thommes, M. and K. A. Cychosz (2018). Recent Advances in the Textural Characterization of Hierarchically Structured Nanoporous Materials. *ECS Meeting Abstracts*, **MA2018-01**(41); 2374

Thommes, M., K. Kaneko, A. V. Neimark, J. P. Olivier, F. Rodriguez-Reinoso, J. Rouquerol, and K. S. W. Sing (2015). Physisorption of Gases, with Special Reference to the Evaluation of Surface Area and Pore Size Distribution (IUPAC Technical Report). *Pure and Applied Chemistry*, **87**(9–10); 1051–1069

Trejo-Zárraga, F., F. de Jesús Hernández-Loyo, J. C. Chavarría-Hernández, and R. Sotelo-Boyás (2018). Kinetics of Transesterification Processes for Biodiesel Production. In K. Biernat, editor, *Biofuels - State of Development*. InTech, London, pages 149–179

Tsai, C.-H. and W.-T. Tsai (2024). Sustainable Processes Reusing Potassium-Rich Biomass Ash as a Green Catalyst for Biodiesel Production: A Mini-Review. *Processes*, **12**(12); 2736

Verma, P., Y. Kuwahara, K. Mori, R. Raja, and H. Yamashita (2020). Functionalized Mesoporous SBA-15 Silica: Recent Trends and Catalytic Applications. *Nanoscale*, **12**(21); 11333–11363

Walkowiak, A., L. Wolski, O. I. Lebedev, M. Daturi, and M. Ziołek (2024). Unraveling the Impact of Phosphate Doping on Surface Properties and Catalytic Activity of Gold Supported on Mixed Iron-Niobium Oxide in Gas Phase Methanol Oxidation. *Journal of Catalysis*, **434**; 115504

Wang, Q., Y. Liu, K. Chen, W. Zhang, J. Li, et al. (2024). Pore Engineering in Biomass-Derived Carbon Materials for Enhanced Energy, Catalysis, and Environmental Applications. *Molecules*, **29**(21); 5172

Widianingsih, S., I. Yanti, A. Kamari, and I. Fatimah (2024). Thermal Conversion of Coral Waste and Its Utilization as Low-Cost Catalyst for Biodiesel Production. *Science and Technology Indonesia*, **9**(4); 866–875

Yaakob, Z., I. S. B. Sukarman, B. Narayanan, S. R. S. Abdullah, and M. Ismail (2012). Utilization of Palm Empty Fruit Bunch for the Production of Biodiesel from *Jatropha curcas* Oil. *Bioresource Technology*, **104**; 695–700

Zahan, K. A. and M. Kano (2019). Technological Progress in Biodiesel Production: An Overview on Different Types of Reactors. *Energy Procedia*, **156**; 452–457

